

PAPER

Stability and normal zone propagation in YBCO CORC cables

To cite this article: M Majoros *et al* 2016 *Supercond. Sci. Technol.* **29** 044006

Manuscript version: Accepted Manuscript

Accepted Manuscript is “the version of the article accepted for publication including all changes made as a result of the peer review process, and which may also include the addition to the article by IOP Publishing of a header, an article ID, a cover sheet and/or an ‘Accepted Manuscript’ watermark, but excluding any other editing, typesetting or other changes made by IOP Publishing and/or its licensors”

This Accepted Manuscript is © © 2016 IOP Publishing Ltd.

During the embargo period (the 12 month period from the publication of the Version of Record of this article), the Accepted Manuscript is fully protected by copyright and cannot be reused or reposted elsewhere.

As the Version of Record of this article is going to be / has been published on a subscription basis, this Accepted Manuscript is available for reuse under a CC BY-NC-ND 3.0 licence after the 12 month embargo period.

After the embargo period, everyone is permitted to use copy and redistribute this article for non-commercial purposes only, provided that they adhere to all the terms of the licence <https://creativecommons.org/licenses/by-nc-nd/3.0>

Although reasonable endeavours have been taken to obtain all necessary permissions from third parties to include their copyrighted content within this article, their full citation and copyright line may not be present in this Accepted Manuscript version. Before using any content from this article, please refer to the Version of Record on IOPscience once published for full citation and copyright details, as permissions will likely be required. All third party content is fully copyright protected, unless specifically stated otherwise in the figure caption in the Version of Record.

View the [article online](#) for updates and enhancements.

Stability and normal zone propagation in YBCO CORC cables

M. Majoros¹, M. D. Sumption¹, E. W. Collings¹ and D. van der Laan²

¹Center for Superconducting & Magnetic Materials (CSMM), The Ohio State University,
Columbus, OH, USA

²Advanced Conductor Technologies and University of Colorado, Department of Physics,
Boulder, CO, USA

Abstract

In this work, a two layer CORC (Conductor On Round Core) cable was tested for stability and Normal Zone Propagation (NZP) at 77 K in a liquid nitrogen bath. The cable was instrumented with voltage taps and wires on each strand over the cable’s central portion (i.e. excluding the end connections of the cable with the outside world). A heater was placed in the central zone on the surface of the cable, which allowed pulses of various powers and durations to be generated. Shrinking (recovering) and expanding (not recovering) normal zones have been detected, as well as stationary zones which were in thermal equilibrium. Such Stationary Thermal Equilibrium zones (STE) did not expand or contract, and hit a constant upper temperature while the heater current persisted; they are essentially a form of Stekly stability. Overall, the cable showed a high degree of stability. Notably, it was able to carry a current of $0.45I_{c \text{ cable}}$ with maximum temperature of 123 K for one minute without damage.

Introduction

High field superconducting magnets require a large number of ampere-turns. To avoid large self-inductances in such magnets they must be wound using superconducting cables. Compared to other currently available high-temperature superconducting (HTS) cables [1 – 10], CORC cables [11] – [14] (see figure 1) have a circular cross-section and the strands of which they are composed are helically twisted around the former. This makes them very suitable for the winding of superconducting magnets. Stability and normal zone propagation (NZP) is crucial in magnet applications. Indeed, NZP is a key parameter determining the magnet's quench protection scheme. In the present paper we measured NZP and more generally quench evolution in a 156 cm long, 2-layer CORC cable operating in a liquid nitrogen bath at 77 K. During these measurements we tested both cool-down and warm-up cycles, as well as allowable over-currents.

Samples

The YBCO tape used in the cable was 4 mm wide and had a nominal critical sheet current density of 25 A per 1 mm of tape width in self-field at 77 K. This results in cable nominal critical current of 600 A (77 K, self-field). The tape was stabilized by a 20 μ m thick copper layer that was plated around the tape. The outside dimensions of the Cu-plated tape cross-section were 4.1 mm in width and 100 μ m in thickness. Within the cable the tapes were wound helically with their superconducting layer on the inside, i.e. facing the former, to take advantage of their ability to sustain relatively large axial compressive strain without mechanical damage [11] – [14]. The cable used a flexible 5.5 mm diameter segment of stranded copper as the former; the former was insulated from the tapes. The two layers in the cable were wound with opposite chiralities (helicities). No interlayer insulation was used which allowed some level of current

sharing between the tapes in the cable. The voltage wires were wound helically along the tapes and placed in the gaps in between them. The parameters of the CORC cable are summarized in Table 1, and the instrumentation of the cable is shown in figure 2. Voltage taps and wires used in the measurements were positioned on each tape over the central portion of the cable (69 cm long, section $Vx-2$ in figure 2b). They covered only the superconducting portion of the cable, excluding the resistive joints on both ends of the cable. A heater ($42\ \Omega$, 5 mm x 5 mm) was placed on top of the cable, positioned in the middle of its length. The tapes were soldered onto the surface of the conical-shaped copper terminals, with their superconducting layer on the inside, using In-Bi-Sn solder (figure 2b).

Experimental

First we measured the room temperature resistances of each tape in the cable, as determined from the cable current. These results, shown in Table 2, can be used to estimate the cable temperature during NZP experiments above the T_c (90 K) of the YBCO tapes. In case of a stationary NZ they can provide input parameters for equation (2). Using the copper cross-section of the tape and neglecting the contribution of the Hastelloy substrate and buffer layers to the conductivity, we obtain for the tape resistance at room temperature a value of 69.9 m Ω (per cable section 69 cm long, figure 2b)). A parallel connection of six such tapes should have a resistance of 11.65 m Ω . From Table 2 we see that only tapes in the outer layer of the cable (tape 4, 5, 6) show resistances close to 11.65 m Ω . Tapes from the inner layer of the cable (tape 1, 2, 3) show significantly lower resistances which might indicate a possible current sharing with the cable copper former. For evaluation of the temperature of the cable above T_c (= 90 K) we used the calculated value of the cable room temperature resistance (11.65 m Ω) to calibrate the

1
2
3 temperature resistance of the cable above 90 K. Temperatures obtained by this procedure are
4 indicated in the figures (where applicable) throughout the paper.
5
6

7
8 The I - V curves of the tapes in the cable were measured using a sensitive Keithley
9 nanovoltmeter in self magnetic field. NZPs were measured using a multi-channel high-speed
10 data acquisition (DAQ) card controlled via LabView software. Heat was generated by applying a
11 current pulse in the resistive heater. The heater, positioned on the outer surface of the cable
12 (figure 2a), allowed pulses of various powers and durations to be generated at a cable current,
13 during which we applied some percentage of the cable's self-field critical current. During and
14 after the heat pulse NZP was measured by DAQ card.
15
16
17
18
19
20
21
22
23
24
25
26

27 Results and discussion

28
29 The self-field, DC I - V curves of the individual tapes vs. cable current are shown in figure
30 3. Critical currents (determined at the electric field criterion of $1 \mu\text{V}/\text{cm}$) obtained from them are
31 summarized in Table 3. The average cable critical current is $\langle I_c \rangle = 315 \text{ A}$. The maximum I_c is
32 441.51 A (Table 3) which is also the cable critical current. This represents 73.6 % of the cable
33 nominal critical current (600 A). This may be caused partially by the difference in tape self-field
34 compared with the cable self-field or possibly some degradation in winding, handling, or
35 previous measurement. It should be noted that both the I - V curves (Fig. 3) as well as the critical
36 currents obtained from them (Table 3) are determined from the overall cable current, since the
37 currents in individual tapes could not be measured. These numbers reflect the current sharing
38 between individual tapes in the cable, as well as current sharing which is completed within the
39 current lugs of the cable (figure 2). The current sharing between tape 5 and 6 may be responsible
40 for the quasi-linear portions of their I - V curves (between 100 A and 200 A) in figure 3. These
41
42
43
44
45
46
47
48
49
50
51
52
53
54
55
56
57
58
59
60

quasi-linear parts appear prior to a sharp transition around 200 A. On the other hand a significant difference between the critical currents of tapes 2, 4 (all around 300 A) and the critical current of tape 1 and 3 (more than 400 A) and I_c of the tapes 5, 6 (around 200 A) (Table 3, figure 3) may be caused by the current re-distribution within the current lugs of the cable. This current redistribution may be caused by different contact resistances connected in series with the tapes within the cable current lugs [15] measured on the same cable prior to the experiments reported in the present paper. Approximate critical currents of the individual tapes can be estimated as follows. From Fig. 3 and Table 3 we see that tape 5 and 6 have approximately the same critical currents (i.e. $I_{c5} \approx I_{c6}$). Also we may write $I_{c2} \approx I_{c4}$ and $I_{c1} \approx I_{c3}$. If we assume that at 200 A the current is homogeneously distributed among the tapes and the tapes 5 and 6 carry their critical currents, then we obtain $I_{c5} = I_{c6} = 33.33$ A. Similarly if we assume that at 300 A tapes 5 and 6 still carry their critical currents and the rest of the current is homogeneously distributed among the tapes 1, 2, 3 and 4, then we obtain $I_{c2} = I_{c4} = 58.33$ A. Applying the same procedure at 440 A we get $I_{c1} = I_{c3} = 103.33$ A. From this analysis we obtain the cable $I_c \approx 389.98$ A which is not too far away from the measured cable critical current of 441.51 A (Table 3). It represents 88.3 % of the measured cable critical current.

After completing I - V curve measurements we started with experiments on NZP and quench systematics. DC transport currents set to be some percentage of the cable critical current $I_{c \text{ cable}}$ were applied. During and after the heat pulse NZP was measured by a high speed data acquisition card (DAQ) controlled via LabView software. At each DC current I (which was a fraction of the cable critical current) several different experiments were performed with heater pulse currents of different magnitude and duration applied and NZP detected. Combining the heater pulse current magnitude with its duration we were able to detect the onset of the NZP, as

well as watch it either grow or shrink at different ratios of $I/I_{c \text{ cable}}$. This is illustrated in figures 4 – 9.

As seen from figures 4 – 8, the differences between tapes seen in figure 3 do not appear at elevated temperatures. This is in accordance with [15] where it is shown experimentally and by modeling that the current distribution becomes homogeneous when the superconducting tapes transit into their normal state. Tape 1 shows a voltage in the middle of the spread of the data (figure 4 – 8) and tape 5 (figure 6 – 8) shows the lowest voltage.

Figure 4 and figure 5 represent two different regimes of NZs at $I_{cable} = 100$ A. Figure 4 shows a pulse energy high enough to initiate a normal zone, and once the power application is stopped, the zone shrinks – we are in a recovering zone. Figure 5, with a similar power deposition, but a much longer application time (and thus energy) creates a stationary normal zone. This stationary zone is different from a stagnant zone, in that its temperature does not continually increase. It is apparently in thermal equilibrium, such that the power generated by the I^2R in the cable (plus the smaller heater contribution) is exactly matched by the heat removal by the bath. A stagnant zone, on the other hand is spatially confined but has a large and continuing temperature increase, which will lead to burn out. The stationary zone as seen in Figure 5 is relatively benign, and recovers once the power to the heater is switched off. The existence of such a stationary zone phenomenon is essentially a form of Stekly stability, where the heat generation in the conductor is balanced by the heat removal to the cryogen [16]. Looking back to this treatment for LTSC wires, we know that the heat generation per unit length

$$\dot{G} = \rho \frac{I^2}{A_{cu}} \quad \text{and} \quad \dot{Q} = hP(T_m - T_b) \quad (1)$$

Where \dot{G} is the power generation, \dot{Q} is the heat removal, h is the coefficient of heat transfer at the cable to liquid nitrogen boundary, ρ is the stabilizer resistivity, P is the perimeter of the cable, T_m is the maximum temperature reached, A_{Cu} is the cross-section of the cable Cu stabilizer and T_b is the bath temperature. This can be easily solved to find the temperature that the stationary zone will reach

$$T_m = \rho \frac{I^2}{hPA_{Cu}} + T_b \quad (2)$$

Taking an average voltage of 0.8 V from figure 5 and an area of 2-times the heater area, then using eq. (2) and heat transfer coefficient given in [17] we get the temperature of the NZ close to 90 K.

Figure 6 shows an existence of recovering NZ at $I_{cable} = 150$ A, while figure 7 indicates onset of propagating NZ. Here we see that the criterion for stationary zones can no longer be met, and thus the heat generation must be greater than the potential cooling, even given the large temperature margin. Figure 8 represents an onset of NZ creation at $I_{cable} = 200$ A. Figure 9 demonstrates the cable's high degree of stability – the cable was able to carry the current of $0.45I_c$ with maximum temperature of 123 K for 1 minute without damage. It is evident that some tapes (1, 2 and 3) tend to recover while tapes 4, 5 and 6 show a progressive heating. The fact that the tapes 4, 5, and 6 are positioned in outer layers suggest a possibility of additional cooling of tapes 1, 2 and 3 in the inner layer from inside by Cu former.

Minimum energies of shrinking and expanding NZ creation are summarized in Table 4 and a phase diagram of NZ is shown in figure 10. It is seen that there exists a region with no NZ, and the region of a runaway NZ, as expected. In addition, in a narrow region we see a region

1
2
3 labeled recovering or stationary normal zone formation. In that case, short energy pulses will
4
5 lead to recovering zones. Longer pulses may lead to stationary zones, which can be described
6
7 with the Stekly stability approach. These regimes, of course, are strongly dependent upon the
8
9 fraction of the cable current to its critical current (figure 10).
10
11
12
13
14

15 Discussion

16
17 The homogeneous model for current distribution among the tapes gives a lower estimate
18
19 of the temperature (Fig. 9). The maximum voltages in figures 4, 6, 7, 8 are approximately one
20
21 order of magnitude lower than the voltages in figure 9. But all of them are orders of magnitude
22
23 higher than 1 $\mu\text{V}/\text{cm}$ (the I_c criterion). We can assume that in figure 9 the whole cable length is
24
25 in normal state. In figure 9, tapes 4, 5, 6 show the same voltage. These tapes are from the outer
26
27 layer of the cable (in direct contact with LN_2). The inner layer tapes (1, 2, 3) show visibly
28
29 lower voltages. This is in qualitative accordance with Table 2, where the resistances were
30
31 measured at room temperature and at a current of about 1 A, so no thermal inhomogeneities or
32
33 overheatings were present. From Table 2 we see that at 300 K and low currents (1 A) tapes 4, 5,
34
35 6 show significantly higher resistances than tapes 1, 2, 3. We ascribe this to possible some level
36
37 of electrical contact with the cable Cu core. If we assume (in figure 9) that approximately 1/2 of
38
39 the cable current is flowing through tapes 4, 5, and 6 then we obtain a resistance close to 300 K.
40
41 From Table 2 we have the measured resistances on a level of 10 m Ω at room temperature, so it
42
43 can be assumed that they are higher than the resistances in the current lugs. The current lugs are
44
45 more robust than the tapes so the heating effects in the current lugs should not be too high.
46
47
48
49
50
51
52
53

54 If the resistance of the normal zone at T_{max} is much higher than the cable end resistance,
55
56 then even if there are variations in the individual contact resistances, the total circuit resistance of
57
58
59
60

a given tape is controlled by the resistance of the normal region, and the tape currents will tend to be self-balancing. That is, the growth of a normal zone in one tape will tend to cause current redistribution in the cable which is effected (i.e., performed) at the cable current in and out junctions. Or, there is current sharing induced by a normal zone which is actually occurring in the cable junctions. This current sharing is kind of artificial, in that it will be a function of measured cable length. So, some strands of the cable may go normal, while others may be still superconducting. This re-balancing should affect the shape of the voltage vs time graph of a quench. It should be that a single strand going normal should have, (a) in the case of a weakly cooled (conduction, or gas) sample a curvature which is concave up, (b) in the case of a better cooled (LN₂) sample, the curvature, if J_e in the Cu is low enough, and the Stekly conditions can be made to apply, a concave downward curvature, and an eventual saturation, (c) in the case of good cooling and current sharing enabled either along the cable or at the cable ends, an even more concave downward shape, and a saturation level of temperature which is somewhat lower than it would be for inhomogeneous current distribution within the cable.

Conclusion

Recovering as well as non-recovering NZs have been observed in a CORC cable under quench conditions operating in liquid nitrogen and self-field. In addition, for low $I/I_{c \text{ cable}}$, the existence of stationary normal zones in the cable has been seen, which are essentially a form of Stekly stability phenomenon. Several examples of propagating and non-propagating zones were explored at higher $I/I_{c \text{ cable}}$ fractions, and a stability diagram for the cable was generated. The CORC cable in this study showed a high degree of stability. It was able to carry a current of 45

1
2
3 % of the cable critical current with maximum temperature of 123 K for one minute, without
4
5 damage.
6
7

8 9 **Acknowledgements**

10
11 This work was supported by the U.S. Department of Energy, Office of Science, Division of High
12
13 Energy Physics, under Grant DE-SC0011721, DE-SC0007891 and DE-SC0014009.
14
15
16
17
18
19
20
21
22
23
24
25
26
27
28
29
30
31
32
33
34
35
36
37
38
39
40
41
42
43
44
45
46
47
48
49
50
51
52
53
54
55
56
57
58
59
60

References

[1] Takayasu M, Minervini J V, and Bromberg L 2008 Superconductor cable *US Patent Application No.* PCT/US2009/047961

[2] Takayasu M, Chiesa L, Bromberg L, and Minervini J V 2012 *Supercond. Sci. Technol.* **25** 014011

[3] Takayasu M, Mangiarotti F J, Chiesa L, Bromberg L, and Minervini J V 2013 *IEEE Trans Appl. Supercond.* **23** 4800104

[4] Takayasu M, Chiesa L, and Minervini J V 2014 *IEEE Trans Appl. Supercond.* **24** 6600105

[5] Goldacker W, Nast R, Kotzyba G, Schlachter S I, Frank A, Ringsdorf B, Schmidt C and Komarek P 2006 *J. Phys.: Conf. Ser.* **46** 901

[6] Long N J, Badcock R, Beck P, Mulholland M, Ross N, Staines M, Sun H, Hamilton J, and Buckley R G 2008 *J. Phys.: Conf. Ser.* **97** 012280

[7] Lakshmi L S, Staines M P, Badcock R A, Long N J, Majoros M, Collings E W, and Sumption M D 2010 *Supercond. Sci. Technol.* **23** 085009

[8] Terzieva S, Vojenciak M, Pardo E, Grilli F, Drechsler A, Kling A, Kudymov A, Gomory F, and Goldacker W 2010 *Supercond. Sci. Technol.* **23** 014023

[9] Vojenciak M, Grilli F, Terzieva S, Goldacker W, Kovacova M, and Kling A 2011 *Supercond. Sci. Technol.* **24** 095002

[10] Majoros M, Sumption M D, Collings E W, and Long N J 2014 *IEEE Trans Appl. Supercond.* **24** 6600505

[11] van der Laan D C 2009 *Supercond. Sci. Technol.* **22** 065013

[12] van der Laan D C, Lu X F, and Goodrich L F 2011 *Supercond. Sci. Technol.* **24** 042001

[13] van der Laan D C, Goodrich L F, and Haugan T J 2012 *Supercond. Sci. Technol.* **25** 014003

[14] van der Laan D C, Noyes P D, Miller G E, Weijers H W, and Willering G P 2013

Supercond. Sci. Technol. **26** 045005

[15] Willering G, van der Laan D C, Noyes P, Weijers H, Miller G, and Viouchkov Y 2015

Supercond. Sci. Technol. **28** 035001

[16] Stekly Z J J, Thome R, Strauss B, 1969 J. Appl. Phys. **40** 2238.

[17] Majoros M, Sumption M D, Collings E W and van der Laan D C, 2014 *Supercond. Sci.*

Technol. **27** 125008

1
2
3
4
5
6
7
8
9
10
11
12
13
14
15
16
17
18
19
20
21
22
23
24
25
26
27
28
29
30
31
32
33
34
35
36
37
38
39
40
41
42
43
44
45
46
47
48
49
50
51
52
53
54
55
56
57
58
59
60

List of Tables

Table 1. Parameters of the CORC cable used in this study.

Table 2. RT resistance of individual tapes.

Table 3. I_c for individual tapes (315 A average).

Table 4. Deposited energies for different NZ types.

Table 1. Parameters of the CORC cable used in this study.

Cable	Former	Cable ID (mm)	No. layers	No. tapes/layer	Total No. tapes	L_p (mm)
CORC	Cu, stranded, insulated	5.5	2, not insulated	3, not insulated	6	32

1
2
3
4
5
6
7
8
9
10
11
12
13
14
15
16
17
18
19
20
21
22
23
24
25
26
27
28
29
30
31
32
33
34
35
36
37
38
39
40
41
42
43
44
45
46
47
48
49
50
51
52
53
54
55
56
57
58
59
60

Table 2. RT resistance of individual tapes.

Tape	Resistance (mΩ)
1	1.56
2	2.67
3	8.75
4	10.56
5	10.55
6	10.55

Table 3. I_c for individual tapes (315 A average).

Tape	I_c (A)
1	441.51
2	337.35
3	441.51
4	349.35
5	213.34
6	199.90
Max.	441.51
	$= I_{c \text{ cable}}$

1
2
3
4
5
6
7
8
9
10
11
12
13
14
15
16
17
18
19
20
21
22
23
24
25
26
27
28
29
30
31
32
33
34
35
36
37
38
39
40
41
42
43
44
45
46
47
48
49
50
51
52
53
54
55
56
57
58
59
60

Table 4. Deposited energies for different NZ types.

I_{cable}/I_c	Max. energy - no NZ (J)	Min. energy – recovering or stationary NZ (J)	Max. energy, shrinking NZ (J)	Min. energy, expanding NZ (J)
0.226	40.7	42.5	> 8400	
0.34	35.3	37.0	63.5	65.9
0.453	35.3	35.6	35.8	36.0

List of Figures

Figure 1. (a) Two layer CORC cable, 156 cm long, used in the experiments. (b) A detail view of a section of the cable.

Figure 2. (a) Instrumentation of the cable (photo), (b) Instrumentation of the cable - schematics.

Figure 3. Self-field I - V curves of the cable tapes vs. cable current. Linear portions of I - V curves of tape 5 and 6 (in a range between 100 A – 200 A) may be caused by current sharing among the tapes 5 and 6 within the cable.

Figure 4. NZ with recovery (shrinking NZ): $I_{cable} = 100$ A, $I_{cable}/I_{c\ cable} = 0.226$, $I_{heater} = 1.00$ A/5 s, Deposited energy = 210 J/25mm².

Figure 5. NZ with recovery (*stationary* NZ): $I_{cable} = 100$ A, $I_{cable}/I_{c\ cable} = 0.226$, $I_{heater} = 1.00$ A/200 s, Deposited energy = 8400 J/25mm².

Figure 6. NZ with recovery (shrinking NZ): $I_{cable} = 150$ A, $I_{cable}/I_{c\ cable} = 0.34$, $I_{heater} = 0.55$ A/5 s, Deposited energy = 63.5 J/25mm².

Figure 7. NZ with no recovery (expanding NZ): $I_{cable} = 150$ A, $I_{cable}/I_{c\ cable} = 0.34$, $I_{heater} = 0.56$ A/5 s, Deposited energy = 65.9 J/25mm².

Figure 8. NZ with recovery (shrinking NZ): $I_{cable} = 200$ A, $I_{cable}/I_{c\ cable} = 0.453$, $I_{heater} = 0.412$ A/5 s, Deposited energy = 35.6 J/25mm².

Figure 9. NZ with no recovery (expanding NZ): $I_{cable} = 200$ A, $I_{cable}/I_{c\ cable} = 0.453$, $I_{heater} = 0.414$ A/5 s, Deposited energy = 36.0 J/25mm².

Figure 10. NZ phase diagram.

1
2
3
4
5
6
7
8
9
10
11
12
13
14
15
16
17
18
19
20
21
22
23
24
25
26
27
28
29
30
31
32
33
34
35
36
37
38
39
40
41
42
43
44
45
46
47
48
49
50
51
52
53
54
55
56
57
58
59
60

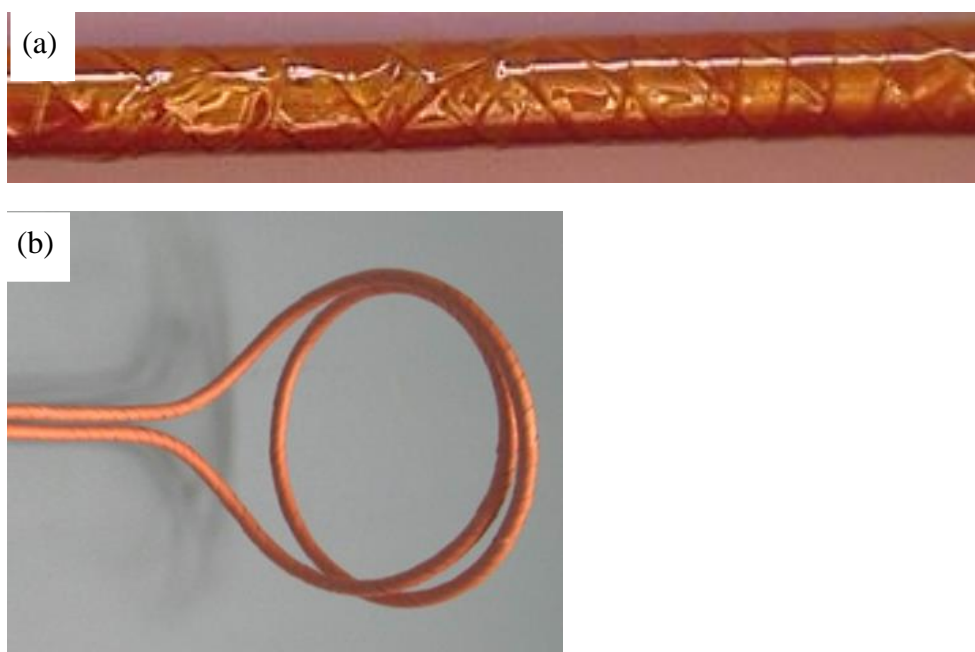


Figure 1. (a) Two layer CORC cable, 156 cm long, used in the experiments. (b) A detail view of a section of the cable.

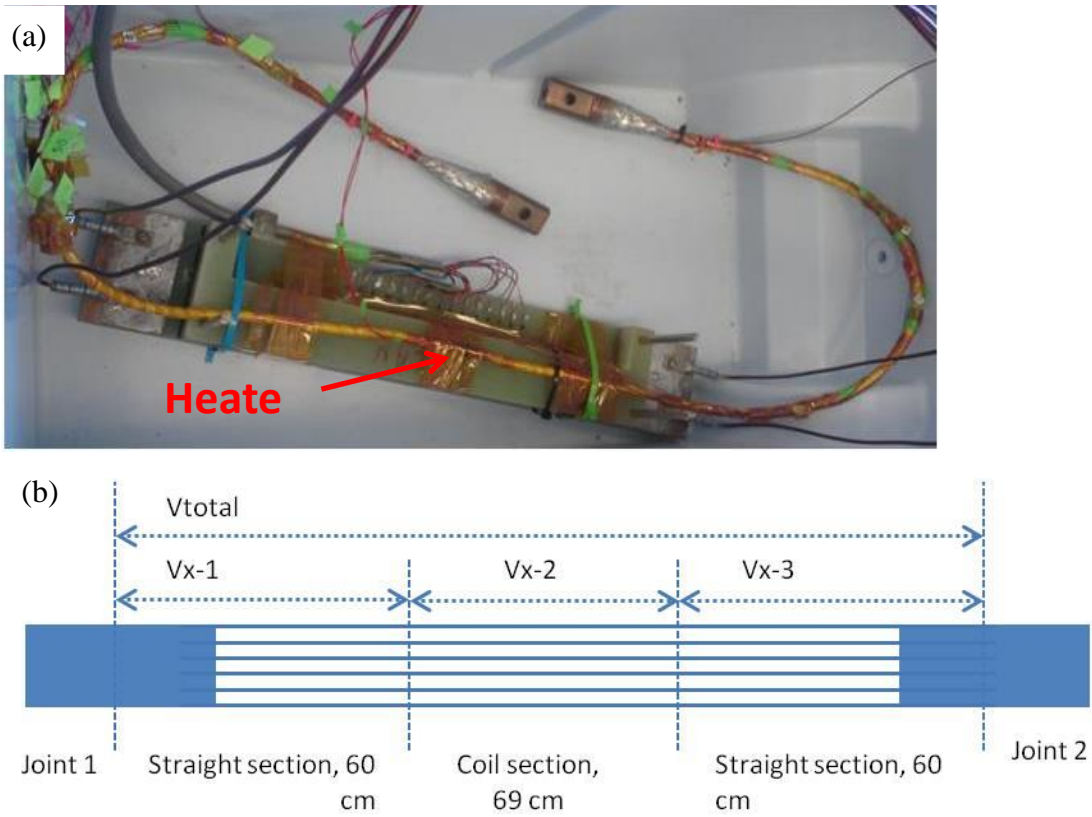


Figure 2. (a) Instrumentation of the cable (photo), (b) Instrumentation of the cable - schematics.

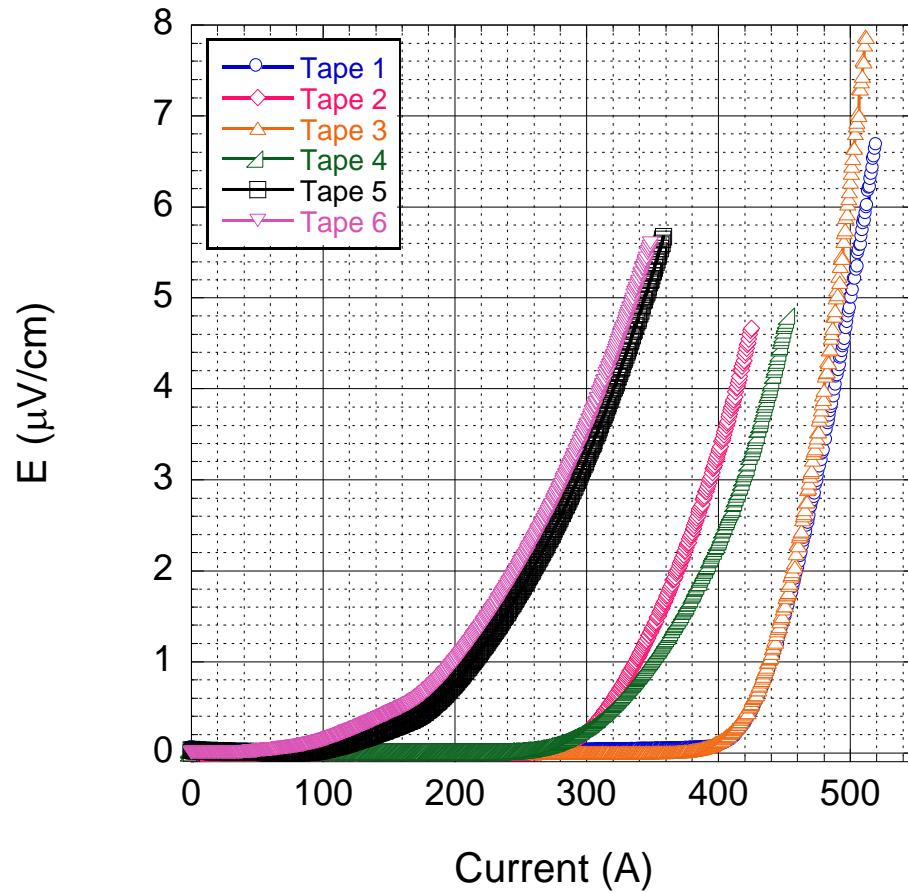


Figure 3. Self-field I - V curves of the cable tapes vs cable current. Linear portions of I - V curves of tape 5 and 6 (in a range between 100 A – 200 A) may be caused by current sharing among the tapes 5 and 6 within the cable.

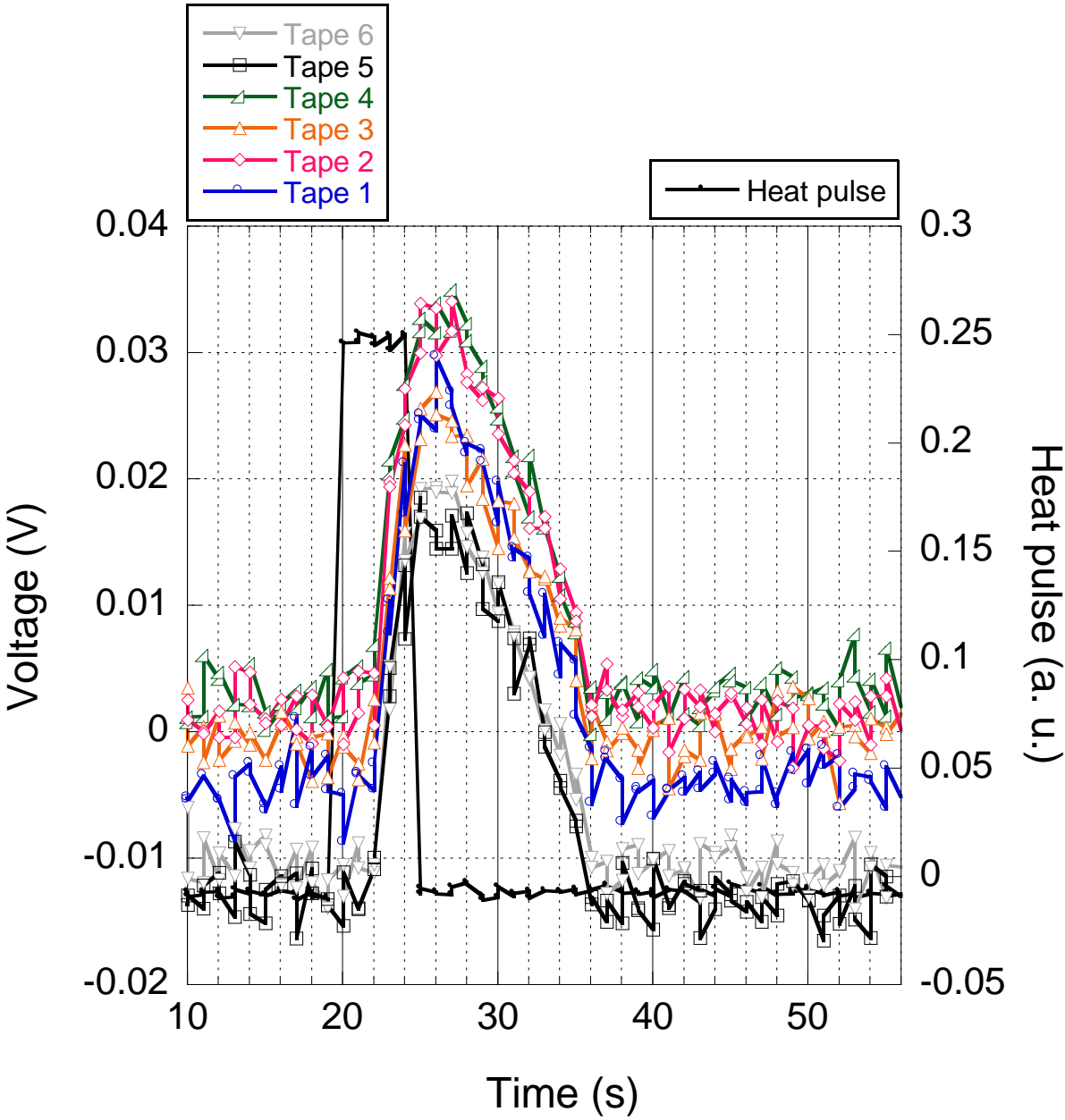


Figure 4. NZ with recovery (shrinking NZ): $I_{cable} = 100\text{ A}$, $I_{cable}/I_{c\text{ cable}} = 0.226$, $I_{heater} = 1.00\text{ A/5}$ s, Deposited energy = 210 J/25mm^2 .

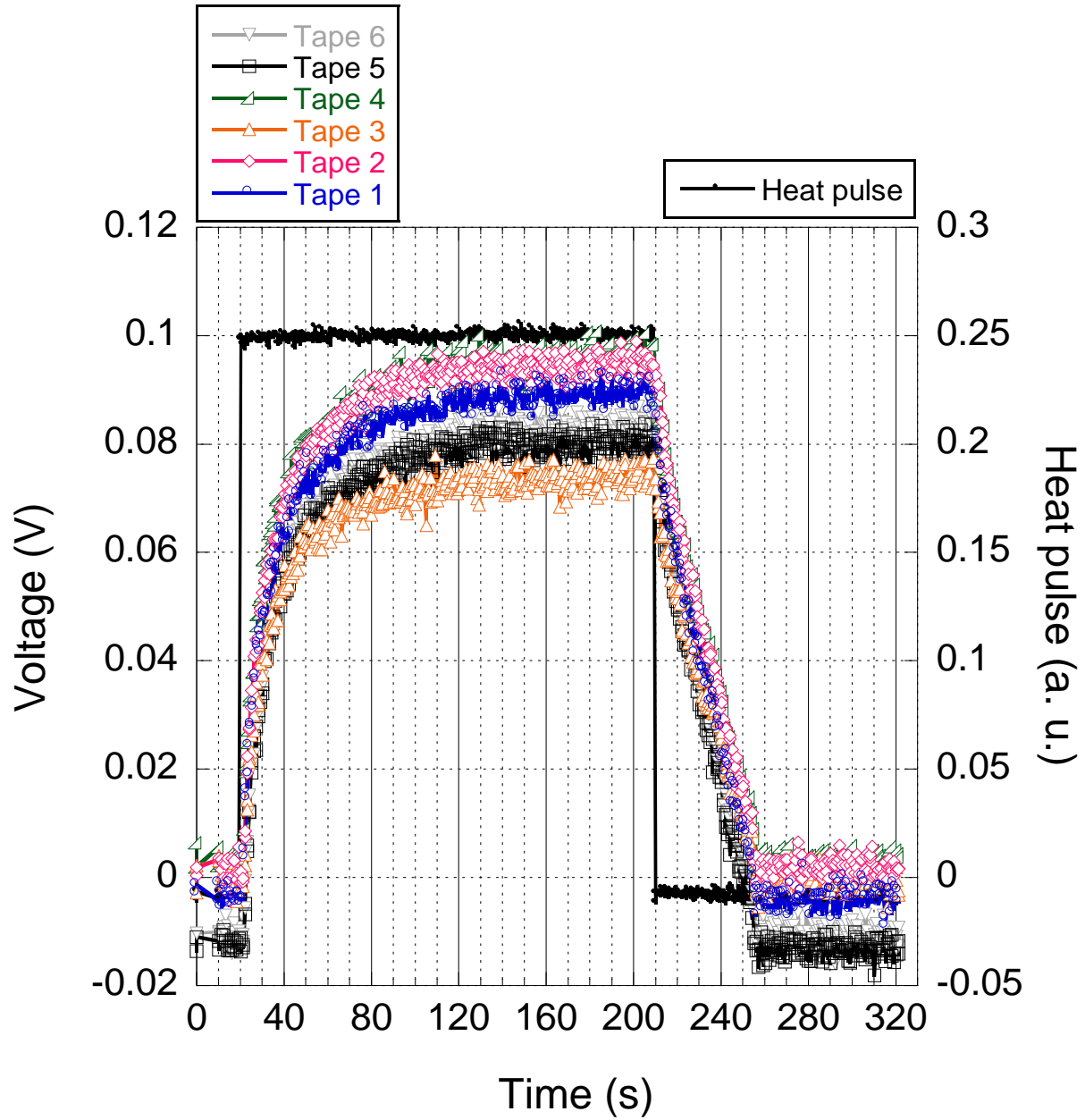


Figure 5. NZ with recovery (*stationary* NZ): $I_{cable} = 100$ A, $I_{cable}/I_{c\ cable} = 0.226$, $I_{heater} = 1.00$ A/200 s, Deposited energy = 8400 J/25mm².

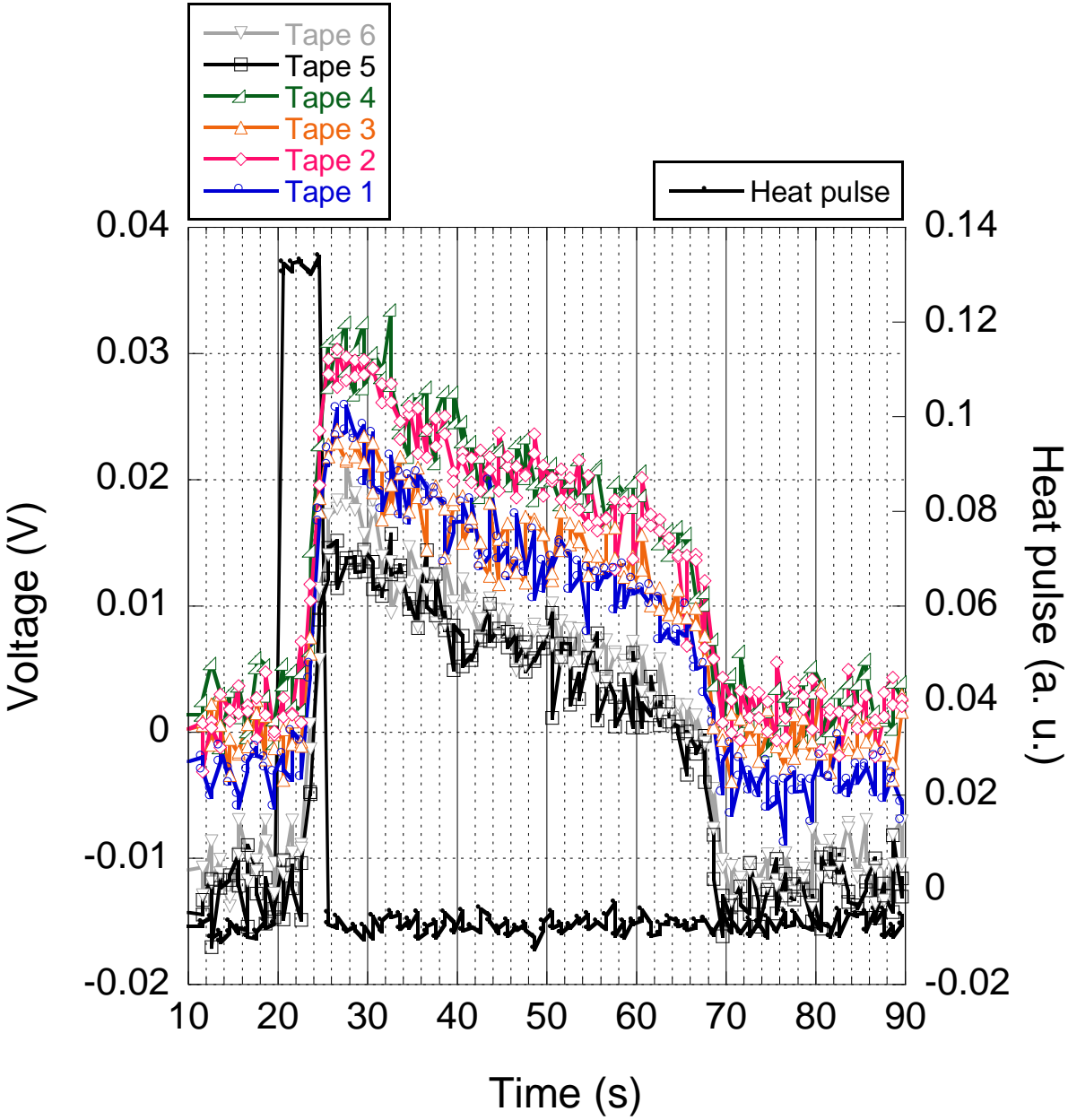


Figure 6. NZ with recovery (shrinking NZ): $I_{cable} = 150$ A, $I_{cable}/I_{c\ cable} = 0.34$, $I_{heater} = 0.55$ A/5 s, Deposited energy = 63.53 J/25mm².

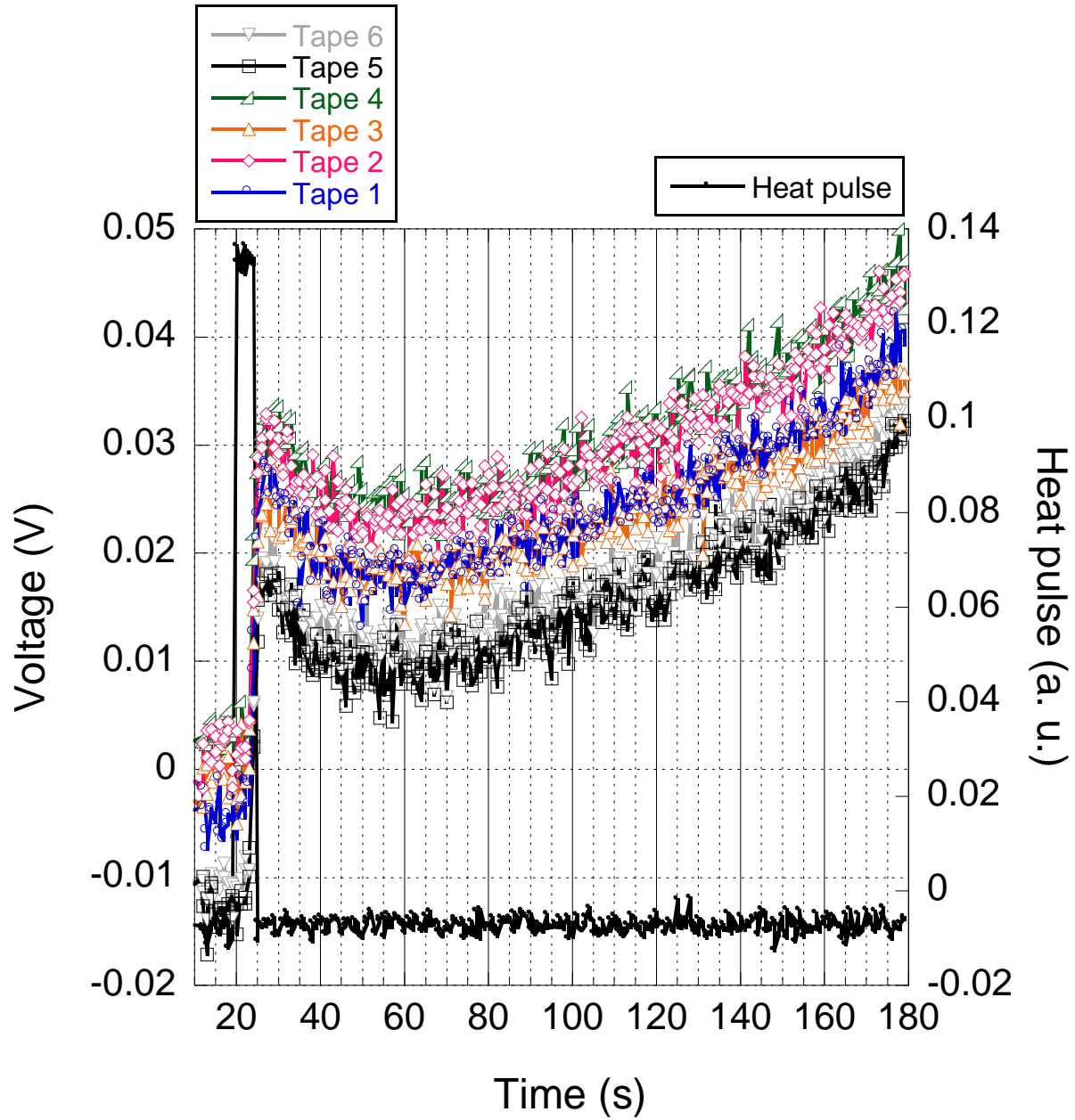


Figure 7. NZ with no recovery (expanding NZ): $I_{cable} = 150$ A, $I_{cable}/I_{c\ cable} = 0.34$, $I_{heater} = 0.56$ A/5 s, Deposited energy = 65.9 J/ 25mm^2 .

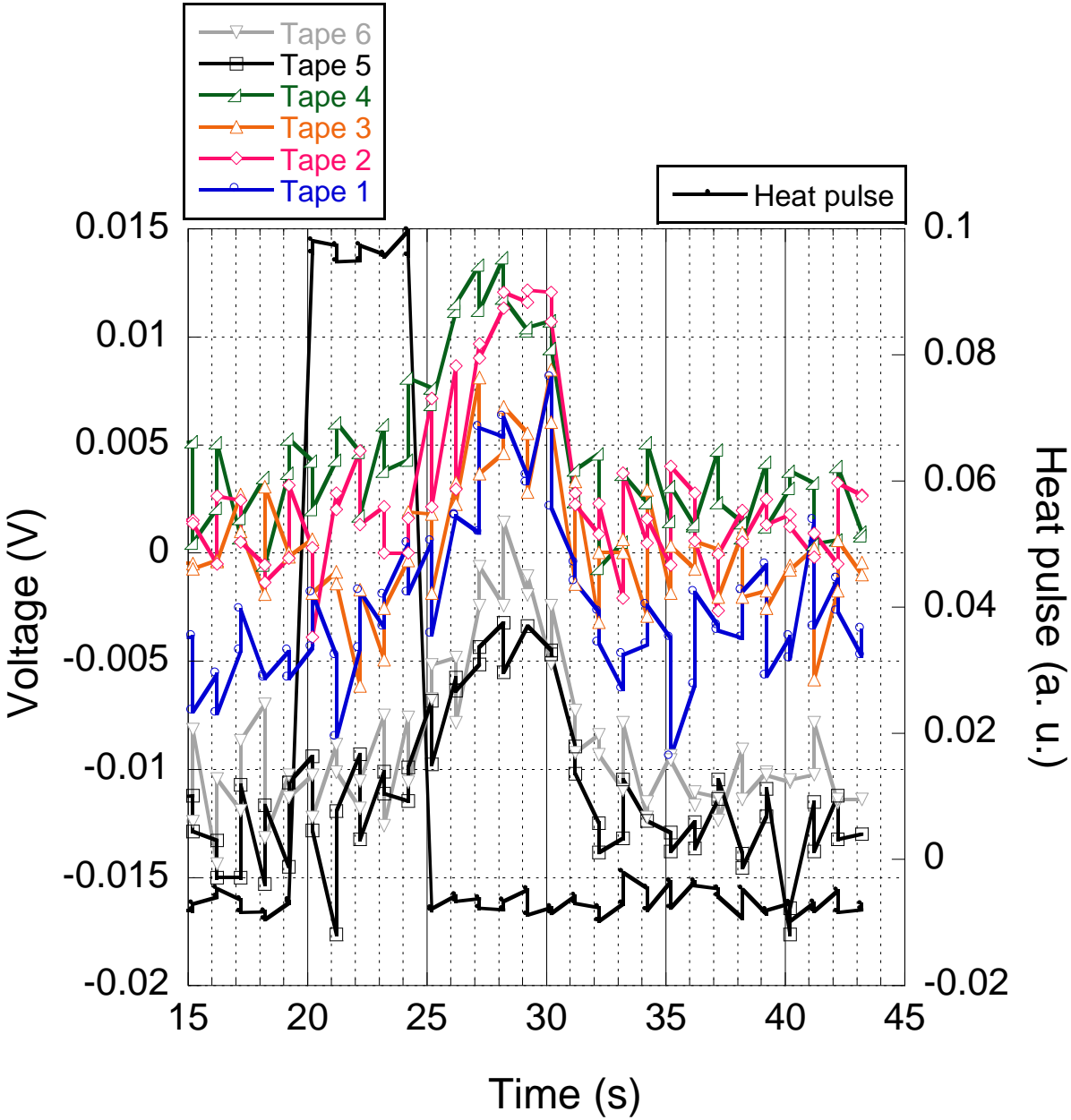


Figure 8. NZ with recovery (shrinking NZ): $I_{cable} = 200 \text{ A}$, $I_{cable}/I_{c \text{ cable}} = 0.453$, $I_{heater} = 0.412 \text{ A/5 s}$, Deposited energy = 35.65 J/25mm^2 .

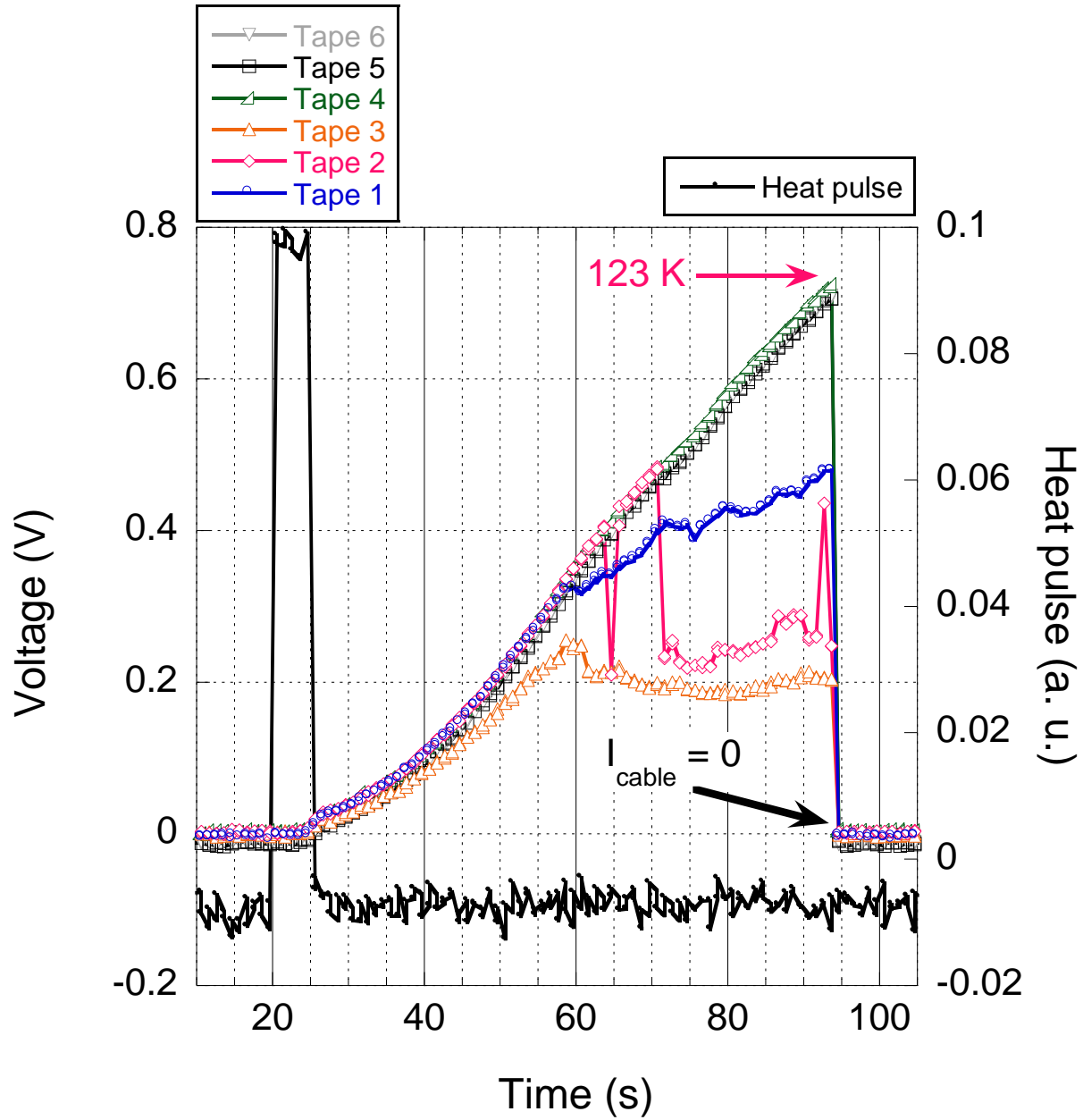


Figure 9. NZ with no recovery (expanding NZ): $I_{cable} = 200$ A, $I_{cable}/I_{c\ cable} = 0.453$, $I_{heater} = 0.414$

A/5 s, Deposited energy = 36.0 J/ 25mm^2 .

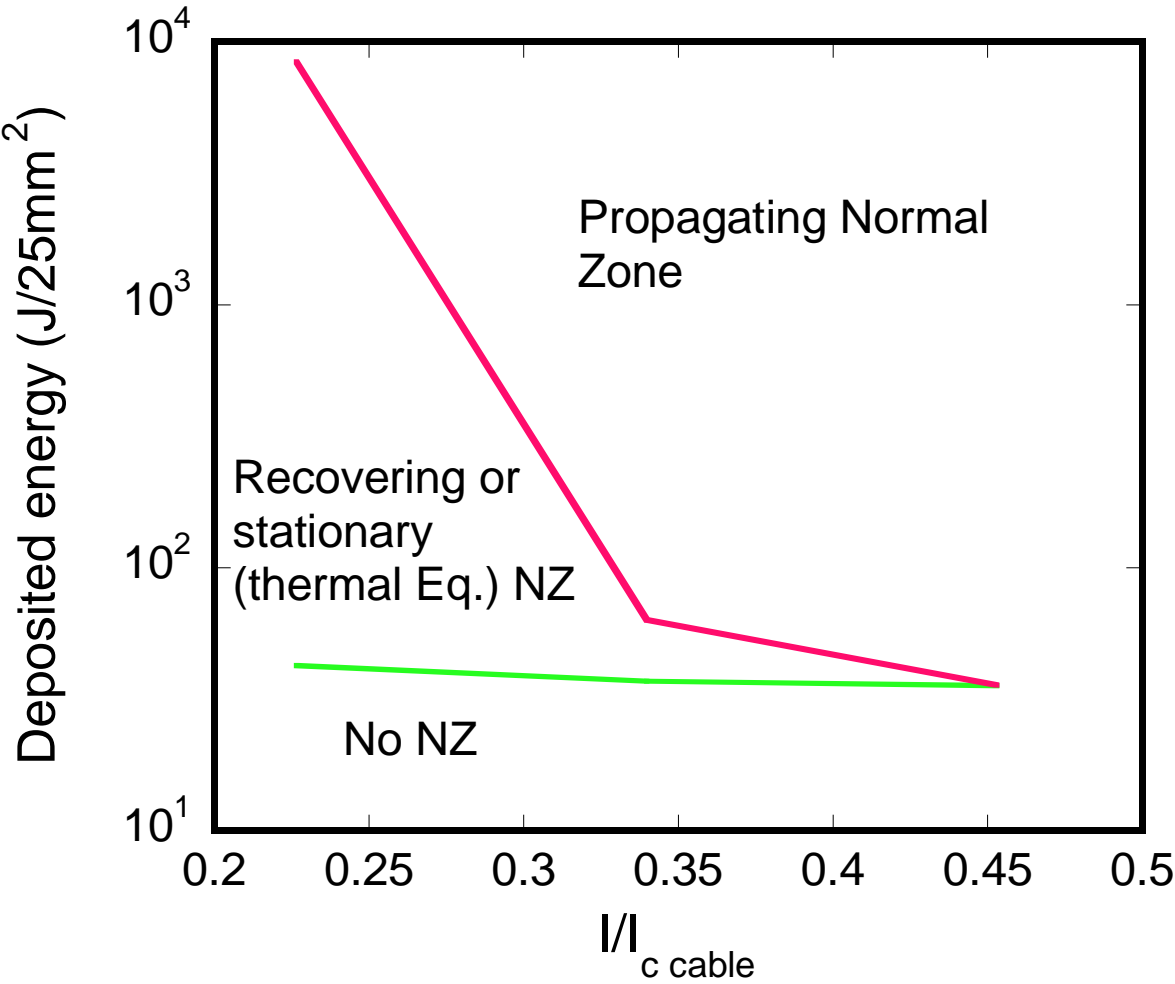


Figure 10. NZ phase diagram.